DMLC tracking and gating can improve dose coverage for prostate VMAT

E Colvill[1,2,3], P R Poulsen[4,5], J T Booth[2,3], R T O'Brien[1], J A Ng[1,3], P J Keall[1]

[1]*Radiation Physics Laboratory, Sydney Medical School, University of Sydney, NSW 2006, Australia*

[2]*Northern Sydney Cancer Centre, Royal North Shore Hospital, Sydney, NSW 2065, Australia*

[3]*School of Physics, University of Sydney, NSW 2006, Australia*

[4]*Department of Oncology, Aarhus University Hospital, Nørrebrogade 44, 8000 Aarhus C, Denmark*

[5]*Institute of Clinical Medicine, Aarhus University, Brendstrupgaardsvej 100, 8200 Aarhus N, Denmark*

Purpose: To assess and compare the dosimetric impact of dynamic multileaf collimator (DMLC) tracking and gating as motion correction strategies to account for intrafraction motion during conventionally fractionated prostate radiotherapy.

Methods: A dose reconstruction method was used to retrospectively assess the dose distributions delivered without motion correction during volumetric modulated arc therapy (VMAT) fractions for 20 fractions of five prostate cancer patients who received conventionally fractionated radiotherapy. These delivered dose distributions were compared with the dose distributions which would have been delivered had DMLC tracking or gating motion correction strategies been implemented. The delivered dose distributions were constructed by incorporating the observed prostate motion with the patient's original treatment plan, to simulate the treatment delivery. The DMLC tracking dose distributions were constructed using the same dose reconstruction method with the addition of MLC positions from linac log files obtained during DMLC tracking simulations with the observed prostate motions input to the DMLC tracking software. The gating dose distributions were constructed by altering the prostate motion to simulate the application of a gating threshold of 3 mm for 5 seconds.

Results: The delivered dose distributions showed that dosimetric effects of intrafraction prostate motion could be substantial for some fractions, with an estimated dose decrease of more than 19% and 34% from the planned CTV $D_{99\%}$ and PTV $D_{95\%}$ values respectively for one fraction. Evaluation of dose distributions for DMLC tracking and gating deliveries showed that both interventions were effective in improving the CTV $D_{99\%}$ for all of the selected fractions to within 4% of planned value for all fractions. For the delivered dose distributions the difference in rectum $V_{65\%}$ for the individual fractions from planned ranged from -44% to

101% and for the bladder $V_{65\%}$ the range was -61% to 26% from planned. The application of tracking decreased the maximum rectum and bladder $V_{65\%}$ difference to 6% and 4% respectively.

Conclusion: For the first time, the dosimetric impact of DMLC tracking and gating to account for intrafraction motion during prostate radiotherapy have been assessed and compared with no motion correction. Without motion correction intrafraction prostate motion can result in a significant decrease in target dose coverage for a small number of individual fractions. This is unlikely to effect the overall treatment for most patients undergoing conventionally fractionated treatments. Both DMLC tracking and gating demonstrate dose distributions for all assessed fractions that are robust to intrafraction motion.

1. INTRODUCTION

Intrafraction prostate motion can result in geometric and dosimetric uncertainties during treatment delivery. Previous studies investigating the dosimetric effects of intrafraction prostate motion show that there is a small drop in dose coverage for treatment fractions with large prostate motion.[1-3] These effects are seen to average out with increased fractionation[2] and over a conventionally fractionated treatment course, the dosimetric effects caused by intrafraction motion are minimal.

To date, intrafraction prostate motion is most commonly managed by addition to treatment margins which results in the surrounding organs at risk receiving an increase in dose to ensure sufficient target coverage. Overcoming the uncertainties due to intrafraction prostate motion is essential to achieve the high accuracy necessary for the safe delivery of hypofractionated and dose escalated treatment courses[3] which have been shown to benefit prostate patients,[4, 5] Localisation systems can now provide the necessary information needed to account for intrafraction prostate motion through motion correction strategies such as CyberKnife[6] and gimbaled linac[7] treatments along with gating, DMLC tracking[8, 9] and dynamic couch tracking.[10]

DMLC tracking for prostate cancer radiotherapy has recently been clinically applied for the first time[8] and as treatments involving motion correction such as gating and DMLC tracking become more widely implemented, the ability to reconstruct the dose delivered during treatment will become increasingly useful as part of the quality assurance process and the clinical workflow within treatment centres. A dose reconstruction method which can be used to assess the dose delivered for DMLC tracking treatments has

been developed and used to assess the potential dosimetric benefit of this motion correction technique.[11, 12] This method along with several other dose reconstruction techniques can be used to retrospectively provide information on the dose delivered during gated and non-gated treatments.[1, 2] To date, however the direct dosimetric benefits of implementing a gating threshold has not be assessed relative to non-gated or DMLC tracking treatment delivery.

The aim of this study was to assess and compare the effectiveness of DMLC tracking and gating as motion correction strategies to account for intrafraction motion during conventionally fractionated volumetric modulated radiotherapy (VMAT/RapidArc) prostate cancer treatments with the intention of further extending this to dose escalated and hypofractionated treatments.

2. METHODS AND MATERIALS

To perform this dose reconstruction study we needed treatment plans and observed prostate motion trajectories for each fraction which were used to create the necessary gated prostate motion trajectories and DMLC tracking MLC position files. These were used to reconstruct the delivered, simulated gating and simulated DMLC tracking doses which were then compared to the planned dose distributions. The basic overview of the method for each fraction can be seen in FIG. 1 Each of these points is discussed below in more detail.

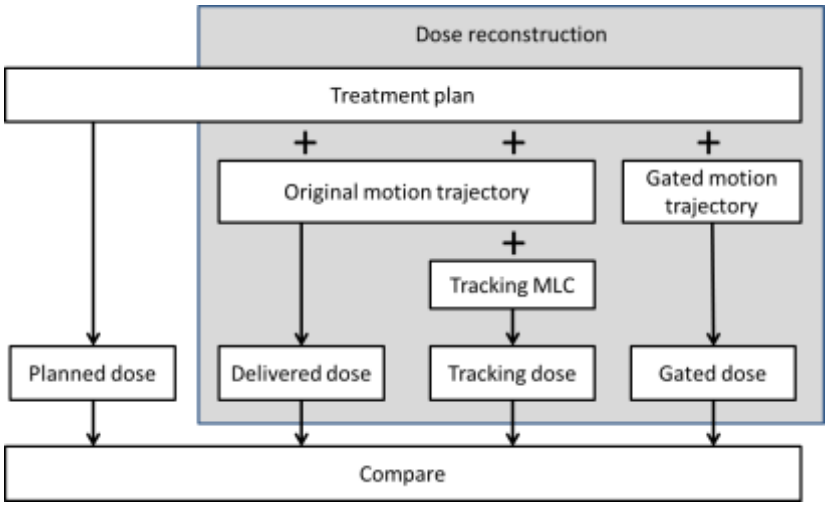

FIG. 1 Overview of dose reconstruction process for each of the selected fractions. The delivered, tracking and gated doses required different input files to construct each distribution. The delivered dose required only the patient treatment plan and

motion trajectory. DMLC tracking dose reconstruction required the addition of tracking MLC positions, acquired through tracking simulations. Gating dose reconstruction required the creation of a simulated gated motion trajectory.

2.A. Prostate motion trajectory and plan selection

The intrafraction prostate motion trajectories in this study were obtained from a previous study and measured using kilovoltage intrafraction monitoring (KIM).[13] In the study, 10 patients with localised prostate cancer were treated using conventionally fractionated VMAT (RapidArc). All patient plans had a CTV to PTV margin of 7 mm with 5 mm posteriorly. Of the 10 patients in the study, we selected the five that would have been eligible for a prospective DMLC tracking clinical trial due to the requirement in our DMLC tracking software that MLC leaves not involved in treatment are placed beneath the jaws. This limits the field size to 14.4 cm, the maximum leaf travel distance on a Millennium MLC. As explained in section 2.C., this involved replanning two patients. From these five patients, there were 135 fractions with measured prostate motion trajectories. From the 135 trajectories we selected 20. Six of these trajectories were selected representing the different categories of translational intrafraction prostate motion previously observed: stable target position, transient excursion, continuous drift, persistent excursion, erratic behaviour and high-frequency excursions.[13, 14] A further 13 trajectories were selected which displayed high mean displacement or which would have resulted in a large number of gating events by exceeding a gating threshold of 3 mm displacement for 5 seconds, as well as trajectories with little motion in order to span the range of clinically observed motion. A frequency histogram of the mean displacement of each of the 135 fractions is shown in FIG 2, where the 20 selected fractions are highlighted in red.

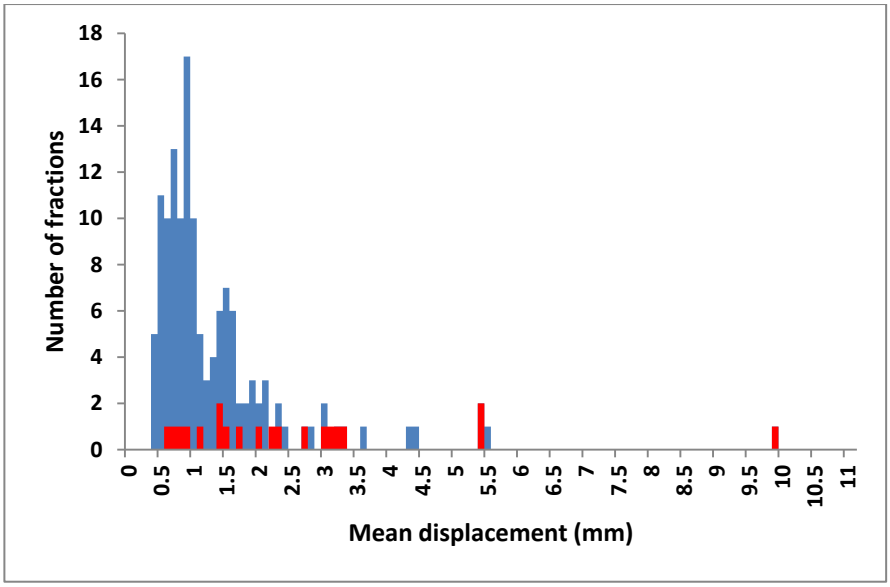

FIG 2 A frequency histogram shows the spread of the mean displacements of the prostate for the 135 observed fractions. The fractions used in this study are highlighted in red.

2.B. Delivered dose reconstruction

The reconstruction of the delivered dose distribution for each of the 20 treatment fractions was performed using an isocenter shift dose reconstruction method[11] and achieved with an in-house Matlab program and an Eclipse (Version 10, Varian Medical Systems, Palo Alto, CA) treatment planning system (TPS). The motion encoding Matlab program incorporates the intrafraction prostate motion trajectory acquired during treatment, with the patient's original treatment plan (pictured in FIG. 3a), exported from the TPS, to create a motion encoded treatment plan which simulates the treatment delivery (FIG. 3b). The motion encoding program divides the intrafraction prostate motion trajectory into 1 mm position bins and for each bin constructs a sub-beam from the original treatment plan control points, representing the arc subtended by the gantry whilst the prostate was within a given position bin. An isocenter shift was used to model the target displacement for each sub-beam.[11] The motion encoded treatment plan is then imported into the treatment planning system and the dose recalculated.

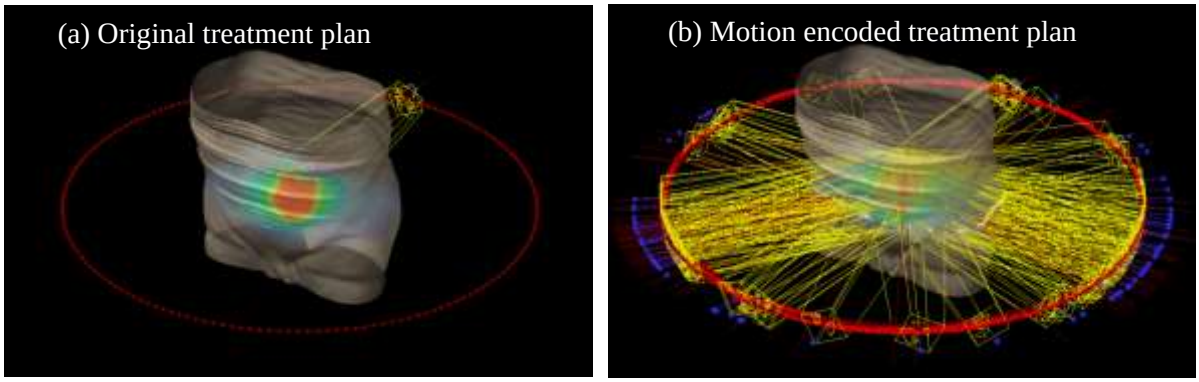

FIG. 3. Pictorial representation of the dose reconstruction method. (a) The patient's original treatment plan with dual VMAT fields (the start of each field is shown by the yellow beam shape, with control points represented by red dots). This original treatment plan is time synchronized with the prostate motion to create (b) a motion encoded treatment plan which has a large number of sub-beams with start positions in yellow. Each sub-beam has a different isocenter, representing a different prostate displacement and is comprised of a varying number of control points (red dots) depending on the amount of time the prostate was in the position corresponding to the isocentre shift of the sub-beam.

2.C. Tracking dose reconstruction

The reconstruction of the dose distributions which would be achieved with the implementation of DMLC tracking differs from that of the delivered and gated dose reconstruction only in that it uses the treatment MLC positions, taken from the linear accelerator log (Dynalog) file, rather than the MLC positions of the original treatment plan. This is necessary because the MLC positions of DMLC tracking treatments are unknown prior to treatment because they are dependent on the target motion.

In order to perform DMLC tracking simulations to obtain the tracking MLC positions, it was necessary to adapt the patients' treatment plans to allow for DMLC tracking. The patients' original VMAT treatment plans have the collimator jaws placed as close as possible to the edge of the aperture shape to minimize the dose leakage between the leaves inside the treatment field. DMLC tracking treatment delivery involves the repositioning of the MLC aperture so that it moves to follow the moving target. For this reason, it is necessary to widen the collimator jaws so that the change in MLC position calculated by the DMLC tracking software does not cause the aperture to move beneath the collimator jaws which would result in a hold of the treatment beam.

Each of the five patients eligible for DMLC tracking had their treatment plans adapted for the purpose for DMLC tracking implementation which involved extending out each of the collimator jaws 8 mm, adding a total of 16 mm to the width of the treatment field in both the x and y direction. These

adapted plans were used for the DMLC tracking simulations only; original plans were used for all dose reconstruction calculations. The maximum width of the treatment field in the x direction (parallel to the leaf motion direction) is dictated by the length of the leaves themselves with the MLC carriage separation limited to 144 mm. The maximum distance between the x jaws is 140 mm. This limitation does not exist for the y jaws (perpendicular to the leaf motion) which can be extended to 400 mm. Two of the five patient plans with the addition of 16 mm exceeded the width limit on the x jaws. For these two patients it was necessary to replan and optimise their treatments with the same objectives of the original plan and with the collimator rotated 90 degrees, prior to extending the collimator jaws. These newly created rotated collimator plans were used for all dose reconstruction calculations for these two patients.

DMLC tracking simulations performed to obtain the Dynalog files containing the tracking MLC positions involved the delivery of the tracking adapted treatment plans, with extended collimator jaws, along with the DMLC tracking software. The observed prostate motion for each fraction was used as real-time motion input into the DMLC tracking software which calculated the new MLC position and sent it to the MLC controller. The linac MLC system then created the Dynalog files which replicate the DMLC tracking delivery for each fraction.

The tracking MLC positions are then used in the motion encoding process rather than the planned MLC positions. The static treatment machine parameters such as collimator angle and jaw position are still carried over from the original treatment plan to the created sub-beams in the motion encoded treatment plan.

2.D. Gated dose reconstruction

The reconstruction of the gated dose distribution of each fraction required the creation of new motion trajectory files for each fraction, which represent the intrafraction prostate motion, had the gating threshold of 3 mm for 5 seconds been used and the treatment beam paused to allow a couch shift to align the prostate to its planned position during the fraction delivery. An in-house Matlab program was used to achieve this, with a gating threshold of 3 mm for 5 seconds. This threshold was chosen as it will be used for an upcoming prospective trial. It is a trade-off between treatment accuracy and efficiency and is within those published for prostate values, for example Lin *et al.*[15] and Li *et al.*[1] have been applying 3mm for 30 seconds thresholds clinically for treatments with longer treatment times per fraction than for the VMAT RapidArc treatments in

this study. When the observed motion trajectory (FIG. 4a) exceeded the gating threshold, a couch shift was modelled by returning the trajectories to the isocenter, creating gated motion trajectories.

The gated motion trajectory files (FIG. 4b) were then incorporated with the original patient treatment plan using the dose reconstruction program which creates the gated motion encoded treatment plan. The gated motion encoded treatment plan was then imported into the TPS and the gated dose distribution calculated.

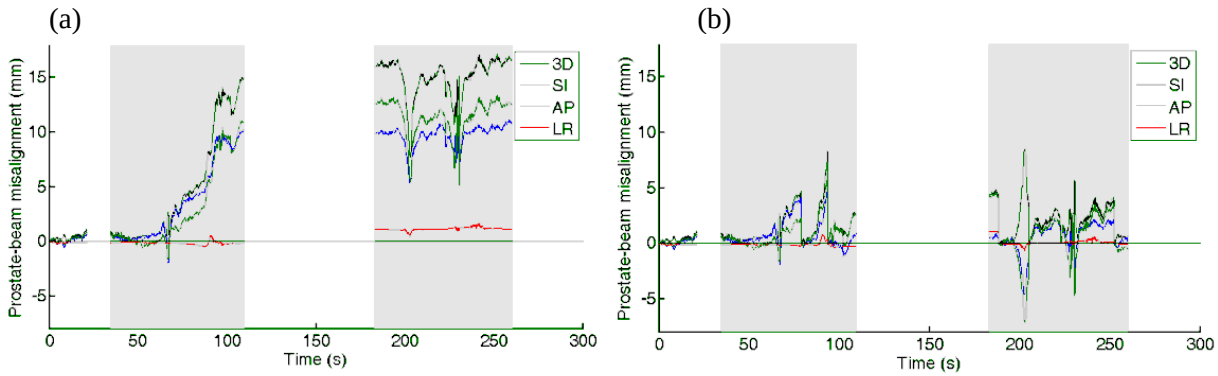

FIG. 4. (a) Observed 3D prostate motion trajectory, grey areas represent treatment beam on. (b) Modified prostate motion trajectory with a gating threshold correcting for motion ≥3mm for ≥5 seconds applied.

2.E. Calculation verification

The dose reconstruction method used for this study has been previously validated using radiographic film measurements.[11] The results of the study showed that for dual-arc VMAT treatment delivery for lung to a thorax phantom with a moving tumor. The reconstructed dose to the target volume closely agreed with the measured dose with a 99.4% and 99.6% gamma pass rate (2 mm/2%) for a moving target delivery with DMLC tracking and without DMLC tracking respectively.[11]

To further validate the method used in the current study an end-to-end experiment was performed using one of the selected fractions (fraction number 3) and a Delta4 (ScandiDos AB, Uppsala) phantom with the Hexamotion programmable 6D motion platform (ScandiDos AB, Uppsala). The patient plan was calculated on the phantom CT within the TPS and then delivered to the phantom setup. For the selected fraction the patient plan was delivered four times: to the static phantom, to phantom programmed to move with the observed prostate trajectory with and without DMLC tracking and to the phantom programmed to move with the gated prostate trajectory (no DMLC tracking). The motion monitoring system for these experiments was the clinical Calypso (Varian Medical Systems, Palo Alto) real-time output which was fed to

the DMLC tracking software. These measurements incorporated the latency of the entire clinical tracking system (measured to be approximately 230 ms). The motion trajectories and Dynalog files obtained for each treatment experiment were used to reconstruct the delivered dose on the phantom CT set within the TPS. The reconstructed doses were then imported into the Delta4 software and compared to the measured doses and a 3D 3 mm/3% gamma pass rate calculated.

The measured dose to the static phantom resulted in a 3 mm/3% gamma pass rate of 100% relative to both the original patient planned dose and the reconstructed static dose. The measured dose delivered to the moving phantom programmed with the observed fraction trajectory resulted in a gamma pass rates of 70.3% (delivered), 98.1% (DMLC tracking) and 97.5% (gating). When comparing each of the delivered dose distributions to that estimated by the dose reconstruction method, the gamma pass rates were 99.8% (delivered), 99.6% (DMLC tracking) and 98.5% (gating). These high gamma pass rates indicate that the calculations represent the measurement conditions with a maximum dose reconstruction error (1.5%) smaller than the effect of the motion itself (29.7%).

The fraction used for the end-to-end experiments was fraction number 3 which was in the 98th percentile of mean displacements for the observed fractions, contained gating events and represents persistent motion. The fraction was not representative of most of the observed fractions, which had much smaller motion, but was selected for its complexity to best verify the dose reconstruction process.

Further verification of the motion encoding method was achieved for this study by creating motion encoded patient treatment plans for each patient using customized motion files with both zero motion representing the motion trajectory, had the prostate not moved from the planned position, and a constant 7 mm motion representing a sustained shift of the prostate in each of the three dimensions of motion.

The zero motion and constant 7 mm motion files were incorporated with the patient's original treatment plan using the motion encoding program. The constant motion encoded treatment plans were then imported into the TPS and the dose distribution calculated. The zero motion dose distribution was then compared to the planned dose distribution and the constant 7 mm constant motion dose distribution was compared to the dose distribution of the original treatment plan with a 7 mm shift applied, in the opposite direction, to the planning isocenter.

Verification of the DMLC tracking dose reconstruction was achieved by obtaining Dynalog files through DMLC tracking simulations using the zero motion and 7 mm shift motion files as input for each patient. The DMLC tracking motion incorporated treatment plans created by encoding the constant motion files and their corresponding Dynalog files was imported into the TPS and compared with the original treatment plan.

For brevity, the constant motion verification results are not shown, however the calculated dose distribution for the zero motion and constant 7 mm treatment plans were exactly the same as the planned and shifted dose distributions for all five patient treatment plans used in the study. The corresponding DMLC tracking dose reconstructions were also the same as all five of the patient's original planned dose distributions.

2.F. Statistical tests

From the dose distributions, dose-volume points for the CTV, PTV, rectum and bladder were computed. The PTV dose was monitored, along with the CTV, as this volume behaves as a CTV with zero margins, moving with the same trajectory as the plan CTV. To determine whether the dose-volume points from reconstructed dose distributions between the planned values and the delivered, gated and DMLC tracking methods were significantly different, e.g. whether the delivered CTV $D_{99\%}$ was significantly different from the planned CTV $D_{99\%}$ values, a two-tailed Wilcoxon rank sum test was used. The Wilcoxon test was chosen over the paired Student's t-test as the population of the DVH points cannot be assumed to be normally distributed. The non-normality of the DVH points was confirmed using the Kolmogorov-Smirnov test (only the MLC tracking bladder $V_{65\%}$ was computed as normally distributed). All statistical tests were performed using Matlab R2013a.

3. RESULTS

The delivered dose distributions showed that dosimetric effects of intrafraction prostate motion were substantial for some fractions. Evaluation of dose distributions for DMLC tracking delivery and gating show that both motion correction strategies would be effective at improving target coverage for the fractions with high mean displacement.

3.A. Individual fraction results

The fraction with the largest mean displacement (fraction number 1, 9.9 mm) has a reconstructed delivered dose distribution that when compared to the planned dose distribution represents a large decrease in target coverage while the gated and DMLC tracking dose distribution increase the coverage to close to that of the plan. The 80% isodose curves for the planned, delivered, gated and DMLC tracking distributions for this fraction are shown in FIG. 5. The delivered dose distribution (FIG. 5b) for this fraction has a cold spot (less than 80% of the prescribed dose) within the center of the target volume, this occurs because the shifts applied to the sub-beams within the dose reconstruction program result in parts of the original highly modulated VMAT plan no longer overlapping each other as originally planned but shifting apart. The distributions for DMLC tracking (FIG. 5c) and gating (FIG. 5d) also have less homogeneous dose coverage due to the same effect where portions of the complex VMAT plan overlap in these reconstructed plans where in the original plan they did not. The DVHs derived from the dose distributions for this fraction are shown in FIG. 6. From the plots we can clearly see a 19% drop in $D_{99\%}$ for the CTV and 34% for the PTV $D_{95\%}$ for the delivered dose reconstruction compared to the planned values. A large increase in dose to the rectum is also evident for this fraction. Improvement in dose coverage with the application of both gating and DMLC tracking brings the $D_{99\%}$ for the CTV to within 1% of the planned value. Application of gating results in the $D_{95\%}$ for the PTV being within 3% of that planned and DMLC tracking brings the PTV $D_{95\%}$ value to within 1% of planned. Similar changes in the dose to the rectum and bladder are also evident between the gating and DMLC tracking plans and the delivered plan.

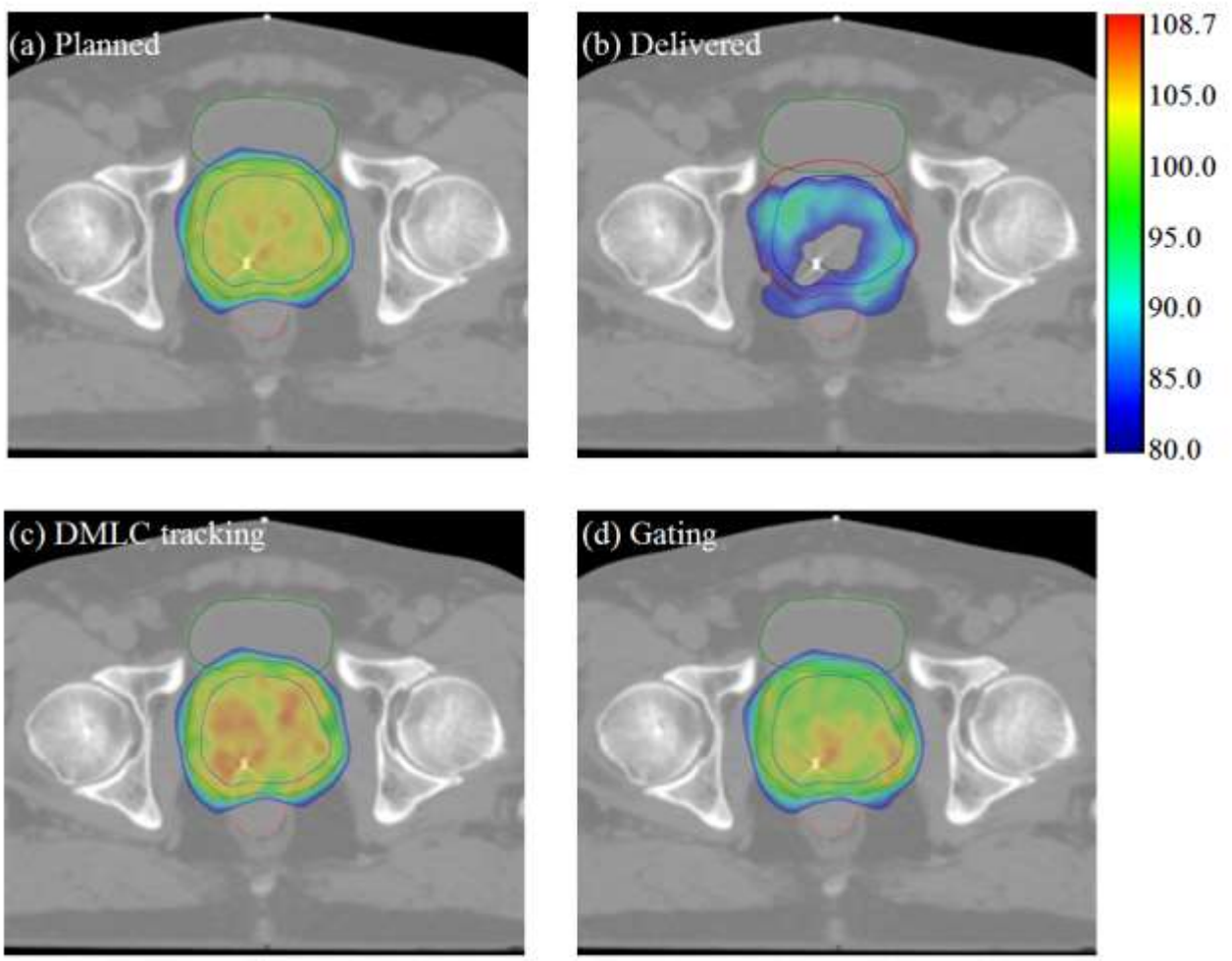

260 **FIG. 5. 80%+ isodose curves for the fraction where the trajectory had the highest mean displacement (a) Planned dose distribution (b) Delivered dose distribution (c) DMLC tracking dose distribution (d) Gated dose distribution. The CTV is contoured blue, the PTV red, the rectum pink and the bladder green.**

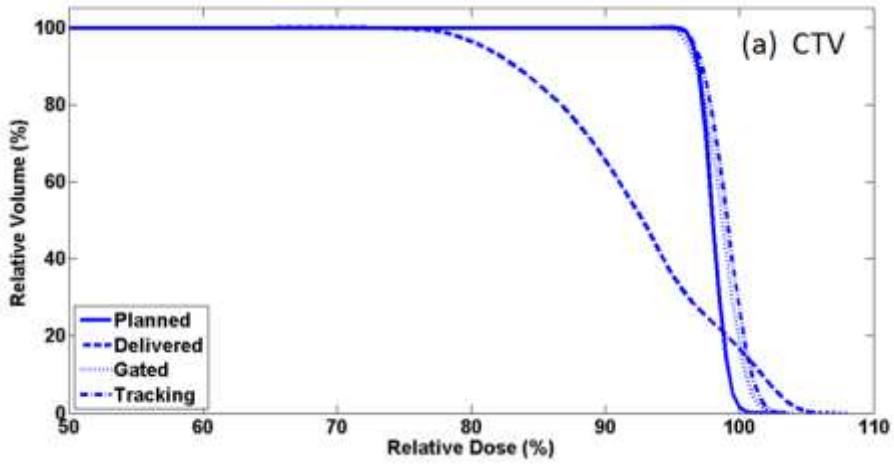

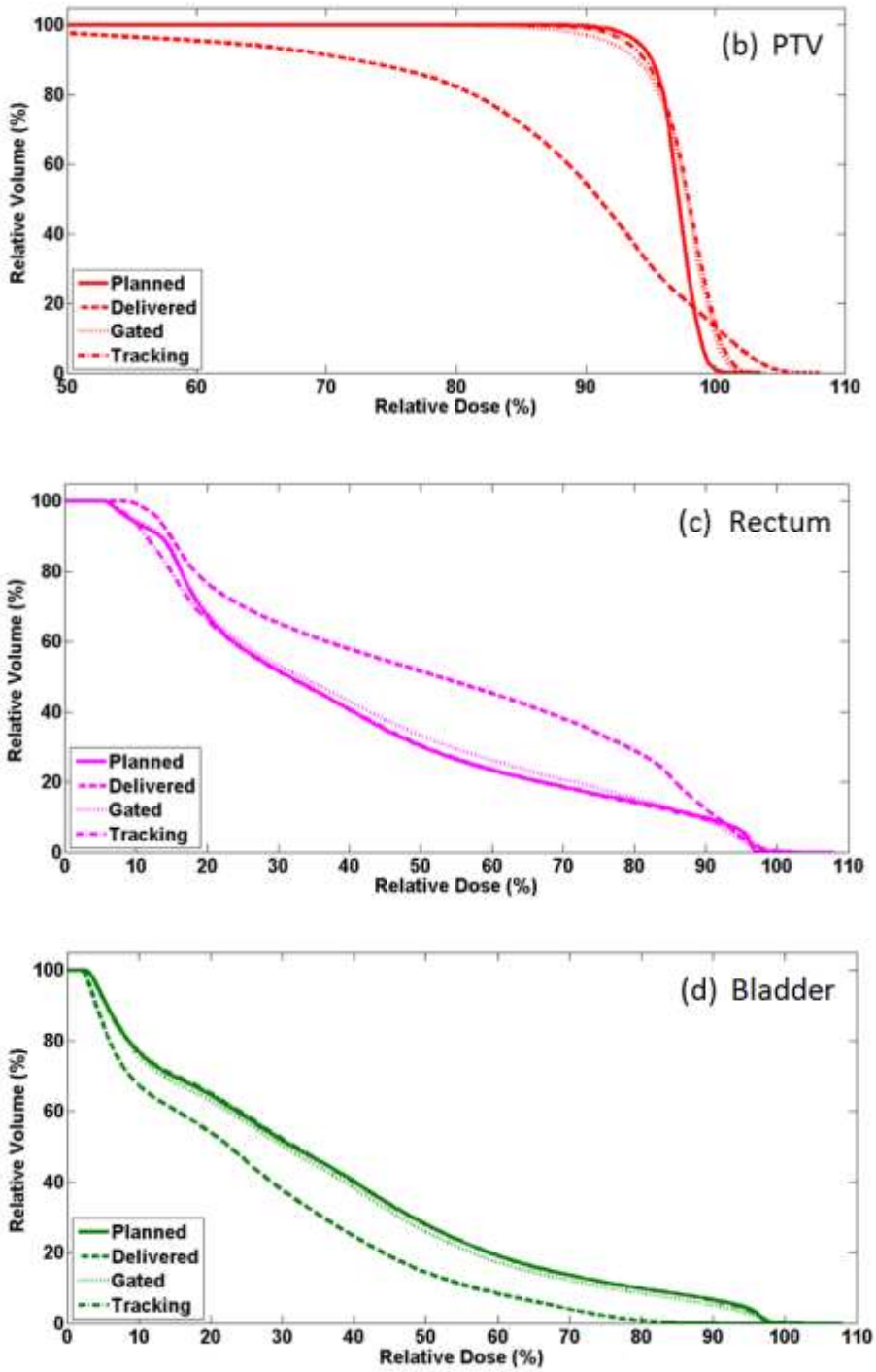

FIG. 6. Set of DVHs comparing the planned (solid), delivered (dashed line), gated (dotted line) and DMLC tracking (dot-dashed line) doses for the fraction with the highest mean displacement. (a) CTV, (b) PTV, (c) rectum and (d) bladder.

3.B. Comparison of multiple fraction results

Table 1 includes the motion type of each of the 20 selected fractions along with the mean (3D) displacement of the fraction and the displacement percentile they fall into for the 135 fractions observed for the five

patients. The percentage difference of the delivered, gated and DMLC tracking dosimetric values from the planned values for the CTV $D_{99\%}$, PTV $D_{95\%}$, the rectum $V_{65\%}$ and the bladder $V_{65\%}$ are also included.

The difference between the planned dosimetric parameters CTV $D_{99\%}$ and PTV $D_{95\%}$, and the delivered dosimetric parameters increases with increasing mean displacement of the motion trajectory which can be seen in FIG 7 as well as Table 1. Motion trajectories of fractions that did not exceed the gating threshold of 3 mm for 5 seconds show smaller variations from the planned $D_{99\%}$ and $D_{95\%}$ values for the CTV and PTV respectively. The difference from the planned dose for all of these fractions is under 3%. Only the fraction in the highest percentile of prostate displacement showed a significant decrease in the CTV $D_{99\%}$ value and only fractions above the 93rd percentile showed a drop of more than 5% to the PTV $D_{95\%}$ value.

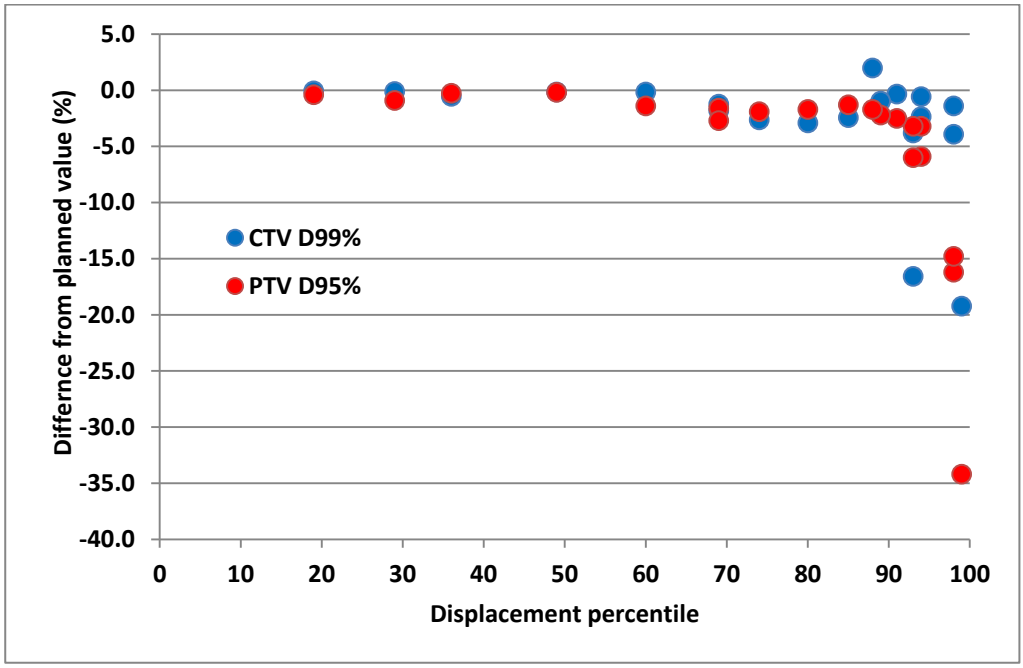

FIG 7. The plot shows the percentage dose difference in CTV $D_{99\%}$ (blue) and PTV $D_{95\%}$ (red) for the delivery distributions for all 20 fractions in the study relative to the mean displacement percentile of each fraction.

Table 1 shows that all of the gated fractions have CTV $D_{99\%}$ and PTV $D_{95\%}$ values within 4% of the planned values. All but two of the fractions (fraction number 5 and 15), which exceeded the gating threshold, had improved PTV dose coverage. These two fractions were characterised by sharp peaks where the modelled gating events did not accurately represent a real-time gate and shift and the resultant gated motion trajectory had a similar mean displacement to the original fraction trajectory. The same trend can be seen in the CTV $D_{99\%}$ values where motions with erratic, transient and persistent motions result in a small decrease in this dosimetric value. Motion trajectories of the fractions which did not exceed the gating

threshold of 3mm for 5 seconds, resulted in the calculated gated dose values being the same as the delivered dose for each of these fractions. The gated dose results for 11 of the 13 fractions with gating events show improvements in the rectum dosimetric parameter $V_{65\%}$ for gating with respect to the delivered value.

The dose distributions that represent what would have been delivered had DMLC tracking been implemented show an improvement in PTV dose coverage compared to the delivered dose distribution calculations for all of the 20 observed fractions. The CTV $D_{99\%}$ for five of the 20 fractions used in this study (fraction numbers 5, 8, 9, 10 and 15) show a decrease with the implementation of DMLC tracking relative to without, this is likely due to combination of the motion types, the highly modulated patient plans and the synchronisation of the motion and treatment delivery during the tracking simulations. The decrease in target dose homogeneity also means that a single dose-volume parameter may not accurately represent the overall dose coverage for the target. The DMLC tracking dose distributions show that this motion correction technique would result in a significant improvement in the $D_{95\%}$ value for the PTV with a p-value of <0.001.

4. DISCUSSION

In this study, time resolved dose reconstruction was performed for 20 representative fractions from five patients to provide dose distributions representing the delivered (without motion correction), gated and DMLC tracking treatments. Substantial variations in the dose distributions were observed in some cases for single fractions without gating or DMLC tracking implementation, which is consistent with findings from previous prostate intrafraction motion dose studies.[1-3, 16] These fractions represent a small percentage of delivered fractions of the five patients in this study and the fractions with smaller (more common) mean displacements show that the margins used were sufficient for target coverage. The large calculated effects of intrafraction motion on the target coverage for individual fractions should have a small effect over an entire conventionally fractionated treatment course as the effect is minimised with increased fractionation.[2] For this reason, the outlier fractions, such as those seen in this study, with a very large decrease in target coverage could have greater implications for hypofractionated treatment courses.

The target coverage of this conventionally fractionated prostate trial was assessed using CTV dose parameters, while the PTV coverage was also monitored as it is representative of a CTV with zero-margins and represents an extreme case. Decreasing the margins from those used in this study would lead to a

dosimetric effect of intrafraction motion on the target somewhere between that of the CTV and PTV in this study.

The 20 fractions used for this study were selected to represent all of the previously observed motion types and the entire range of prostate displacements, 12 of the 20 fractions were selected from top 80th percentile of mean displacement. Of the 13 fractions with intrafraction prostate motion exceeding the gating threshold, five trajectories show a decrease of more than 5% in $D_{95\%}$ for the PTV representing a substantial difference from the dose prescribed.

Previous studies have also investigated and shown the potential dosimetric benefit of DMLC tracking implementation. However, a direct comparison with the dosimetric benefit of implementing a gating threshold has not been investigated. Li *et al.*[1] showed that gating was effective in reducing the mean and maximum intrafraction motion during treatment but the dosimetric effect of gating has not been compared against treatments without motion correction or DMLC tracking treatment techniques. The results of this study show that with the application of either DMLC tracking or gating dose variations from planned target coverage were reduced.

Langen *et al*.[2] performed time-synchronized dose reconstruction for Tomotherapy and step and shoot IMRT using Calypso-measured patient data for 486 fractions from 15 patients. Their study did not include gating or DMLC tracking. Their key findings were that only 4% of the fractions showed >1% CTV D_{95} dose reduction, and that there was no correlation between the motion and dosimetric consequences. Their findings differ from the 'delivered' results in our study, in which greater dose reductions in the CTV were observed, despite the margin (7 mm, 5 mm posterior) being larger than the Langen study (5 mm, 3 mm posterior). Our results also show that both the PTV and CTV dose reduction are highly correlated (-0.97 and -0.85 respectively) with the mean displacement. The differences between the studies could be due to the different patient populations, measurement methods and delivery methods, as well as the potential selection bias in that most of the fractions selected in our study (Table 1) were in the upper range of the mean displacement percentiles.

A study performed by Pommer *et al.*[12] investigated the dosimetric benefits of DMLC tracking using time resolved dose reconstruction for IMAT prostate treatments. The study used fractions representative of a range of intrafraction motions and showed that for fractions with a mean displacement of greater than 3 mm

DMLC tracking would be effective in improving the dose to the target relative to the delivered non-DMLC tracking dose. The results of our study are consistent with these previous results with the DMLC tracking dose calculations showing an improvement on the dose delivered without motion correction with all CTV $D_{99\%}$ values for all 20 fractions within 4% of the planned dose (Table 1).

Li *et al.*[1] investigated the effects of intrafraction prostate motion using a dose convolution reconstruction method on Calypso data for 1267 fractions from 35 patients treated with step and shoot IMRT. The patients were treated in three different groups: a group without motion correction, gate and shift with a 3 mm for 30 seconds threshold and a gate and shift with a 5mm for 30 second threshold. They found that more than 20% of patients had a displacement of more than 3 mm for 5% of the treatment time and that motions of greater than 10 mm were observed to occur but were infrequent. The study showed that applying gating thresholds reduced the mean and maximum displacements of treatment fractions for a patient cohort compared to the group which had no motion correction applied. The study did not however directly show the dosimetric effectiveness of applying a gating threshold, as it is not possible to know the motion, and therefore the dose distributions, that would have been delivered for the two gating groups had the motion correction not been applied. The results of our current study (Table 1) show that the gated dose calculations for a threshold of 3 mm for 5 seconds represent an improvement on that of the delivered dose distributions with all CTV $D_{99\%}$ and PTV $D_{95\%}$ values for all 20 fractions studied within 4% of the planned dose.

Study limitations

The time resolved isocenter shift dose reconstruction method used for this study only accounts for rigid translation and does not account for rotation or deformation of the target.[1111] The method has been previously experimentally verified and while it can accurately model the dose to the target, the dose to surrounding organs at risk, which may move independently of the prostate, are less accurately modelled as any positional or volumetric changes to these organs are unknown.

There are several limitations to the DMLC tracking simulations and dose reconstruction processes. During DMLC tracking simulations the beginning of treatment delivery and the start of the motion trajectory input were manually synchronised leading to an offset between the original motion trajectory and the Dynalog tracking MLC positions when these files were combined using the dose reconstruction program. This offset varies between fractions, but is approximately 0.5 seconds and will have a greater effect on the

calculated dose distributions for high frequency excursion and erratic motion trajectories that have sharper gradients of motion. Improving the accuracy of the synchronisation for the tracking simulations would lead to more accurate tracking dose reconstructions.

The application of DMLC tracking requires the collimator jaws to be 8 mm wider in all directions. The effect of this adaptation on the plan is small with an average increase of less than 0.5% to $D_{95\%}$ for the PTV and to a central reference point within the prostate. This effect will necessarily be accounted for during planning for DMLC tracking implementation.

During the gated dose reconstruction process a gating event was represented as an instantaneous perfect couch shift, though in reality a beam hold would have occurred and time taken to adjust the couch and realign the patient. During this time, prostate motion will continue and perfect realignment of the patient would not necessarily be achieved. The fractions number 5 and 15 which exceeded the gating threshold but did not have improved PTV dose coverage through the couch shift were a transient motion and a high frequency motion trajectory. These fractions were characterised by sharp peaks where an instantaneous couch shift did not allow for self-correction of the motion while the treatment beam was not on and the resultant gated motion trajectory had a similar mean displacement to the original fraction trajectory.

In summary, dose coverage for prostate radiotherapy is improved with the application of motion correction with both DMLC tracking and gating for the few fractions with high mean displacement. These findings provide compelling evidence to perform prospective clinical studies on both of these technologies to eliminate outlier fractions with large displacements with the dual goals of improved tumor control and decreased treatment-related side effects.

5. CONCLUSION

For the first time, the dosimetric impact of DMLC tracking and gating to account for intrafraction motion during prostate radiotherapy have been assessed and compared with no motion correction. Without motion correction intrafraction prostate motion can result in a significant decrease in target dose coverage for some fractions; both DMLC tracking and gating demonstrate dose distributions that are robust to intrafraction motion.

Acknowledgements

The authors acknowledge the financial support of an NHMRC Australia Fellowship. Thanks to Esben Worm (Aarhus) who helped set up the dose reconstruction code at the University of Sydney and to Julie Baz for reviewing and improving the clarity of the paper.

References

[1] H.S. Li, I.J. Chetty, C.A. Enke, R.D. Foster, T.R. Willoughby, P.A. Kupellian, T.D. Solberg, "Dosimetric Consequences of Intrafraction Prostate Motion," International Journal of Radiation Oncology*Biology*Physics **71**, 801-812 (2008).

[2] K.M. Langen, B. Chauhan, J.V. Siebers, J. Moore, P.A. Kupelian, "The Dosimetric Effect of Intrafraction Prostate Motion on Step-and-Shoot Intensity-Modulated Radiation Therapy Plans: Magnitude, Correlation With Motion Parameters, and Comparison With Helical Tomotherapy Plans," International Journal of Radiation Oncology*Biology*Physics2012).

[3] J. Adamson, Q. Wu, D. Yan, "Dosimetric Effect of Intrafraction Motion and Residual Setup Error for Hypofractionated Prostate Intensity-Modulated Radiotherapy With Online Cone Beam Computed Tomography Image Guidance," International Journal of Radiation Oncology*Biology*Physics **80**, 453-461 (2011).

[4] D.A. Kuban, S.L. Tucker, L. Dong, G. Starkschall, E.H. Huang, M.R. Cheung, A.K. Lee, A. Pollack, "Long-Term Results of the M. D. Anderson Randomized Dose-Escalation Trial for Prostate Cancer," International Journal of Radiation Oncology*Biology*Physics **70**, 67-74 (2008).

[5] E.E. Yeoh, R.J. Botten, J. Butters, A.C. Di Matteo, R.H. Holloway, J. Fowler, "Hypofractionated Versus Conventionally Fractionated Radiotherapy for Prostate Carcinoma: Final Results of Phase III Randomized Trial," International Journal of Radiation Oncology*Biology*Physics **81**, 1271-1278 (2011).

[6] G. Morgia, C. De Renzis, "CyberKnife in the Treatment of Prostate Cancer: A Revolutionary System," European Urology **56**, 40-42 (2009).

[7] T. Depuydt, T. Gevaert, D. Verellen, K. Poels, M. Duchateau, K. Tournel, T. Reynders, M. De Ridder, "Geometric accuracy of real-time tumor tracking with the gimbal Linac system of the novel VERO SBRT system," Physica Medica **28, Supplement 1**, S10 (2012).

[8] P.J. Keall, E. Colvill, R. O'Brien, J.A. Ng, P.R. Poulsen, T. Eade, A. Kneebone, J.T. Booth, "The first clinical implementation of electromagnetic transponder-guided MLC tracking," Medical Physics **41**, - (2014).

[9] P.J. Keall, A. Sawant, B. Cho, D. Ruan, J. Wu, P. Poulsen, J. Petersen, L.J. Newell, H. Cattell, S. Korreman, "Electromagnetic-Guided Dynamic Multileaf Collimator Tracking Enables Motion Management for Intensity-Modulated Arc Therapy," International Journal of Radiation Oncology*Biology*Physics **79**, 312-320 (2011).

[10] J. Wilbert, K. Baier, C. Hermann, M. Flentje, M. Guckenberger, "Accuracy of Real-time Couch Tracking During 3-dimensional Conformal Radiation Therapy, Intensity Modulated Radiation Therapy, and Volumetric Modulated Arc Therapy for Prostate Cancer," International Journal of Radiation Oncology*Biology*Physics **85**, 237-242 (2013).

[11] P.R. Poulsen, M.L. Schmidt, P. Keall, E.S. Worm, W. Fledelius, L. Hoffmann, "A method of dose reconstruction for moving targets compatible with dynamic treatments," Medical Physics **39**, 6237-6246 (2012).

[12] T. Pommer, M. Falk, P.R. Poulsen, P.J. Keall, R.T. O'Brien, P.M. Petersen, P.M.a. Rosenschöld, "Dosimetric benefit of DMLC tracking for conventional and sub-volume boosted prostate intensity-modulated arc radiotherapy," Physics in Medicine and Biology **58**, 2349 (2013).

[13] J.A. Ng, J.T. Booth, P.R. Poulsen, W. Fledelius, E.S. Worm, T. Eade, F. Hegi, A. Kneebone, Z. Kuncic, P.J. Keall, "Kilovoltage Intrafraction Monitoring for Prostate Intensity Modulated Arc Therapy: First Clinical Results," International Journal of Radiation Oncology*Biology*Physics **84**, e655-e661 (2012).

[14] P. Kupelian, T. Willoughby, A. Mahadevan, T. Djemil, G. Weinstein, S. Jani, C. Enke, T. Solberg, N. Flores, D. Liu, D. Beyer, L. Levine, "Multi-institutional clinical experience with the Calypso System in localization and continuous, real-time monitoring of the prostate gland during external radiotherapy," International Journal of Radiation Oncology*Biology*Physics **67**, 1088-1098 (2007).

[15] Y. Lin, T. Liu, X. Yang, Y. Wang, M.K. Khan, "Respiratory-Induced Prostate Motion Using Wavelet Decomposition of the Real-Time Electromagnetic Tracking Signal," International Journal of Radiation Oncology*Biology*Physics **87**, 370-374 (2013).

[16] K.M. Langen, W. Lu, T.R. Willoughby, B. Chauhan, S.L. Meeks, P.A. Kupelian, G. Olivera, "Dosimetric Effect of Prostate Motion During Helical Tomotherapy," International Journal of Radiation Oncology*Biology*Physics **74**, 1134-1142 (2009).

Table 1. Each of the selected fractions, their characteristic motion, mean displacement, mean displacement percentile, the calculated delivered, tracking and gated values for dosimetric parameters for the CTV, PTV, rectum and bladder relative the planned dosimetric parameter values (100%). P-values compare the dose-volume points for gating and tracking with the delivered dose. The fractions with grey backgrounds did not display any gating events and therefore the gated values equal the delivered values.

Fraction number	Motion Type	Mean Disp. (mm)	Displacement Percentile	CTV D99 (%)			PTV D95 (%)			Rectum V65 (%)			Bladder V65 (%)		
				Delivered	Tracking	Gated	Delivered	Tracking	Gated	Delivered	Tracking	Gated	Delivered	Tracking	Gated
1	Persistent	9.9	99	-19.2	-0.2	-0.7	-34.2	-0.9	-2.7	100.7	-0.3	11.5	-61.4	0.1	-10.8
2	Erratic	5.4	98	-3.9	-1.3	-3.4	-16.2	-1.6	-2.0	66.8	-1.6	-20.2	-38.0	1.7	14.0
3	Persistent	5.4	98	-1.4	-1.1	-2.6	-14.8	0.2	-1.2	16.9	1.5	-1.4	-37.3	-0.1	-1.5
4	Erratic	3.3	94	-0.6	-0.3	-2.0	-5.9	-1.0	-2.0	16.3	4.9	-2.6	23.8	0.6	1.5
5	High Freq.	3.2	94	-2.4	-2.8	-3.5	-3.2	-1.7	-3.3	-44.4	-0.1	2.1	25.9	-0.6	3.1
6	High Freq.	3.1	93	-3.8	-0.9	-3.4	-3.2	-1.1	-2.1	-18.3	0.6	-6.5	19.8	-4.4	5.4
7	Erratic	3.0	93	-16.6	-1.3	-1.2	-6.0	-1.8	-2.1	26.8	-4.4	0.0	-14.4	3.4	1.0
8	Persistent	2.7	91	-0.3	-1.3	-1.7	-2.5	-1.0	-1.6	1.6	-0.7	-1.7	-4.7	-2.2	0.3
9	Erratic	2.3	89	-1.0	-4.0	-2.1	-2.2	-1.3	-1.2	-19.5	-3.6	-11.0	14.3	-2.6	9.5
10	Persistent	2.2	88	2.0	-0.4	0.5	-1.7	0.8	-0.6	29.7	6.2	8.0	-9.0	2.3	-2.3
11	Drift	2.0	85	-2.4	-0.6	0.0	-1.3	-1.1	0.0	-23.4	2.0	-15.5	13.1	-1.2	5.6
12	High Freq.	1.7	80	-2.9	-1.8	-2.9	-1.7	-0.6	-1.7	-10.1	1.4	-10.1	8.9	2.0	8.9
13	Transient	1.5	74	-2.6	-0.9	0.0	-1.9	-0.8	-1.0	7.5	-3.2	-10.5	-4.3	3.6	4.6
14	Drift	1.4	69	-1.8	-1.2	-1.8	-1.6	-0.8	-1.6	-11.1	2.8	-11.1	5.5	-0.2	5.5
15	Transient	1.4	69	-1.2	-1.4	-1.5	-2.7	-0.7	-2.8	-6.6	-0.4	3.1	-4.2	-1.7	-4.0
16	Drift	1.1	60	-0.2	-0.1	-0.2	-1.4	-1.1	-1.4	-14.5	-6.3	-14.5	5.5	0.0	5.5
17	Stable	0.9	49	-0.2	-0.2	-0.2	-0.2	-0.2	-0.2	0.2	-1.8	0.2	9.6	0.8	9.6
18	Stable	0.8	36	-0.5	-0.3	-0.5	-0.3	-0.1	-0.3	-9.1	-4.1	-9.1	2.2	1.0	2.2
19	Stable	0.7	29	-0.1	-0.1	-0.1	-0.9	-0.7	-0.9	-9.0	-5.9	-9.0	1.5	-1.0	1.5
20	Stable	0.6	19	-0.1	-0.3	-0.1	-0.4	-0.4	-0.4	2.6	2.0	2.6	-3.6	-2.4	-3.6
		p-values compared to delivered		-	0.30	0.50	-	<0.001	0.06	-	0.68	0.53	-	0.69	0.71

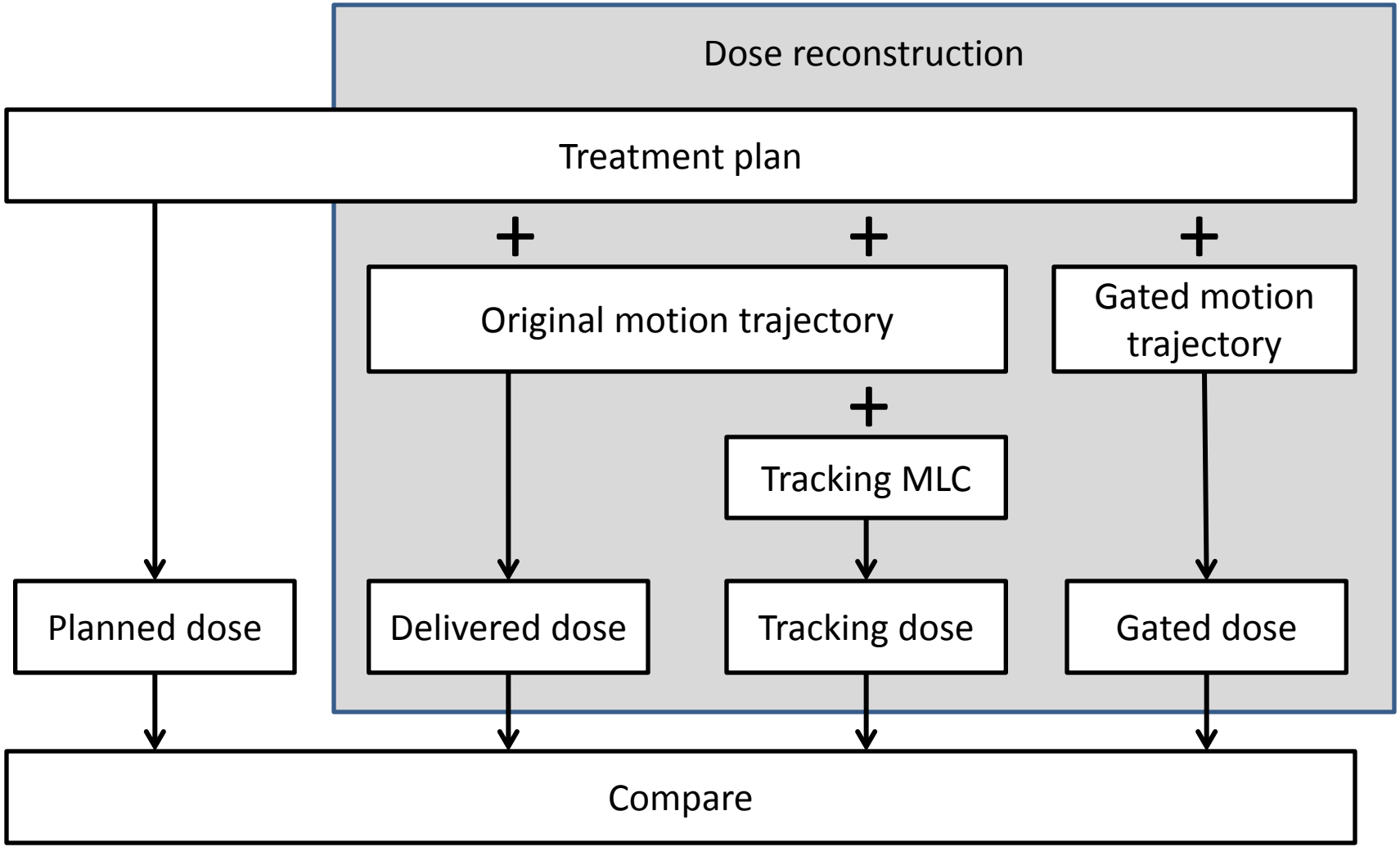
Dose reconstruction
Treatment plan
Original motion trajectory
Gated motion trajectory
Tracking MLC
Planned dose
Delivered dose
Tracking dose
Gated dose
Compare

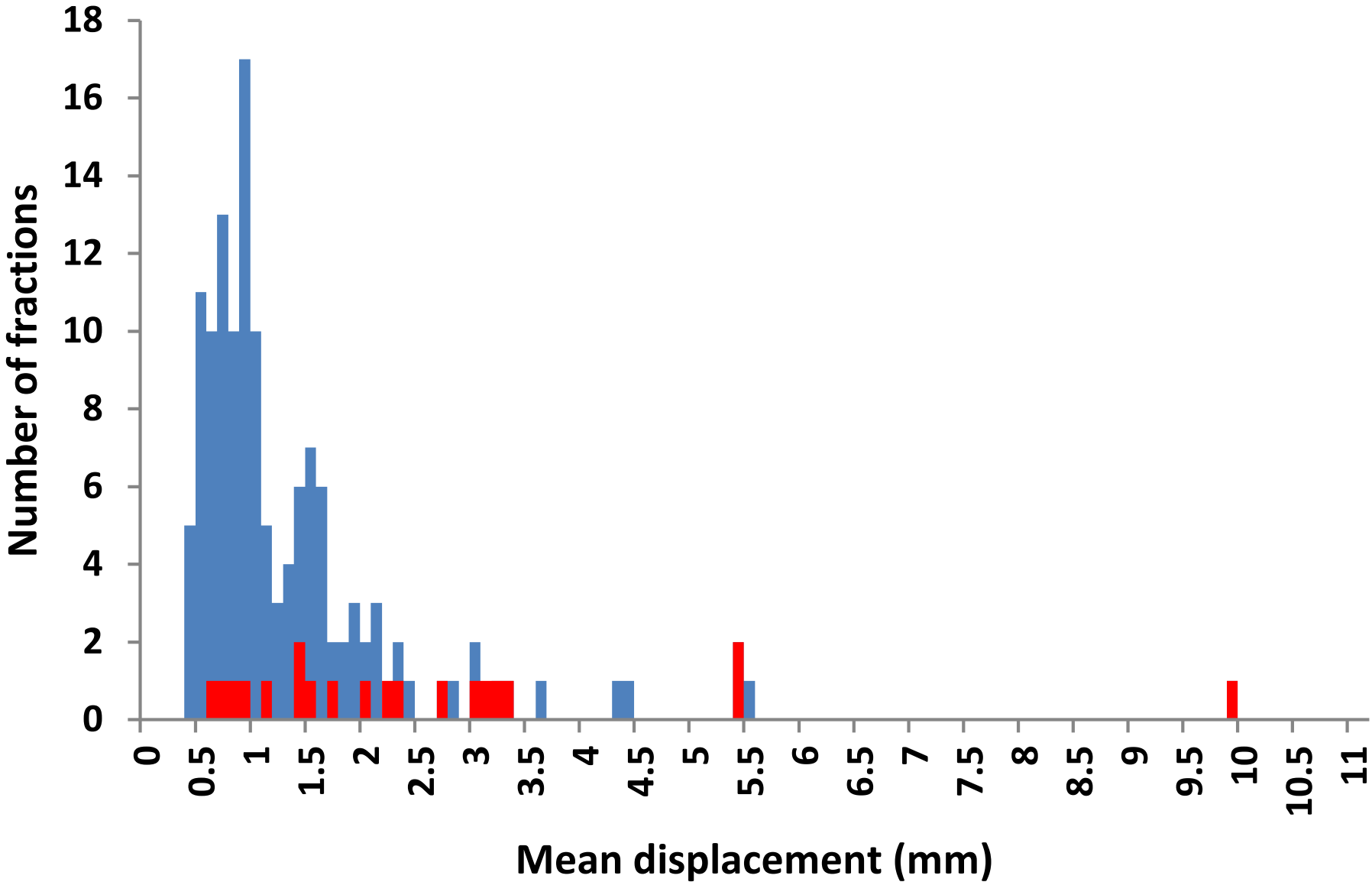
Number of fractions
18
16
14
12
10
8
6
4
2
0
0
0.5
1
1.5
2
2.5
3
3.5
4
4.5
5
5.5
6
6.5
7
7.5
8
8.5
9
9.5
10
10.5
11
Mean displacement (mm)

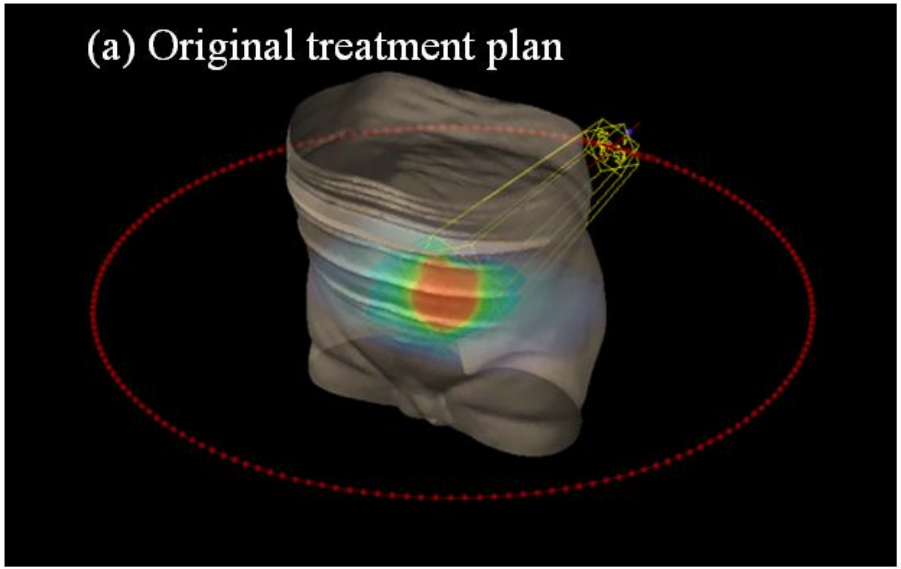
(a) Original treatment plan

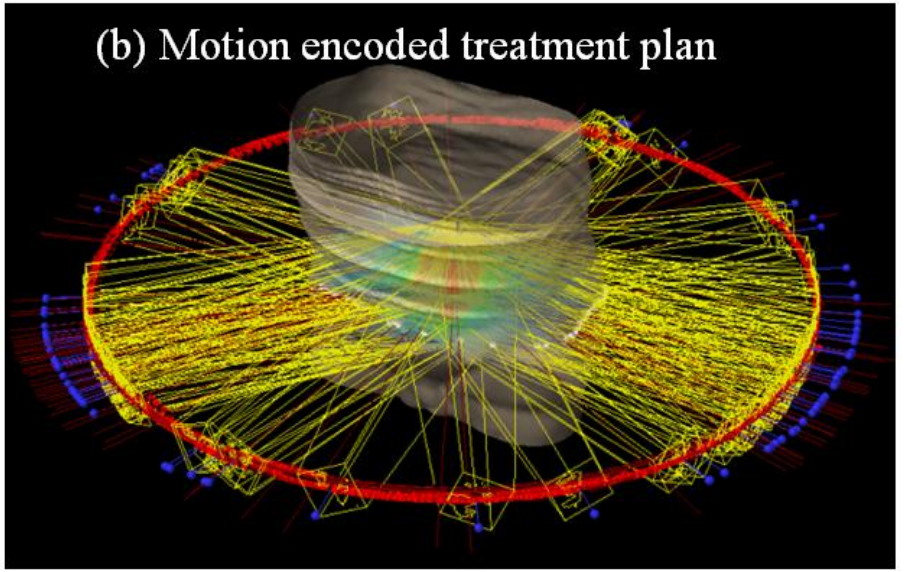
(b) Motion encoded treatment plan

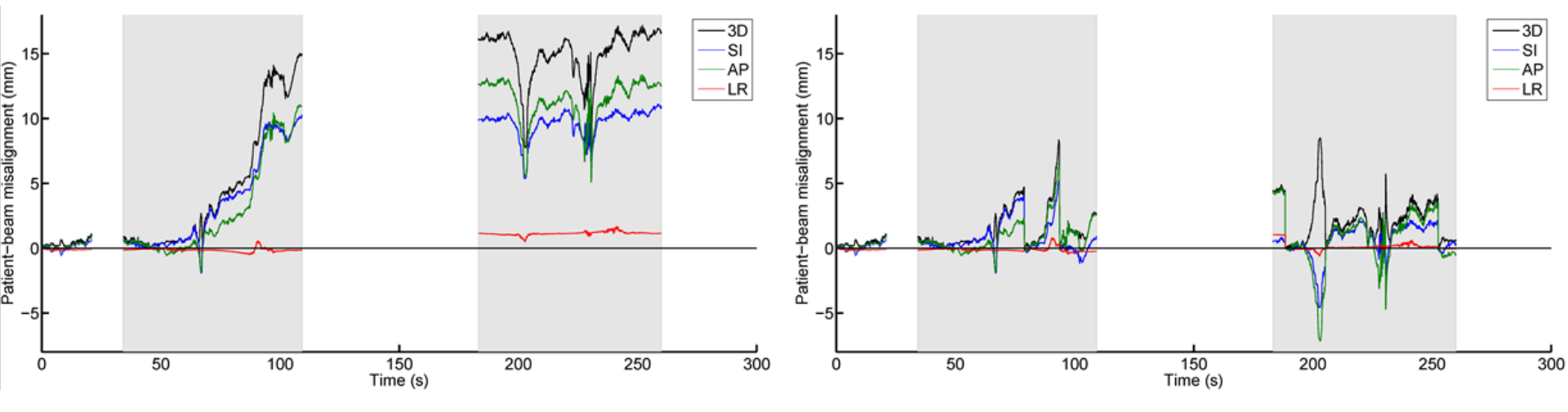
Patient−beam misalignment (mm)
15
10
5
0
−5
0
50
100
150
200
250
300
Time (s)
3D
SI
AP
LR

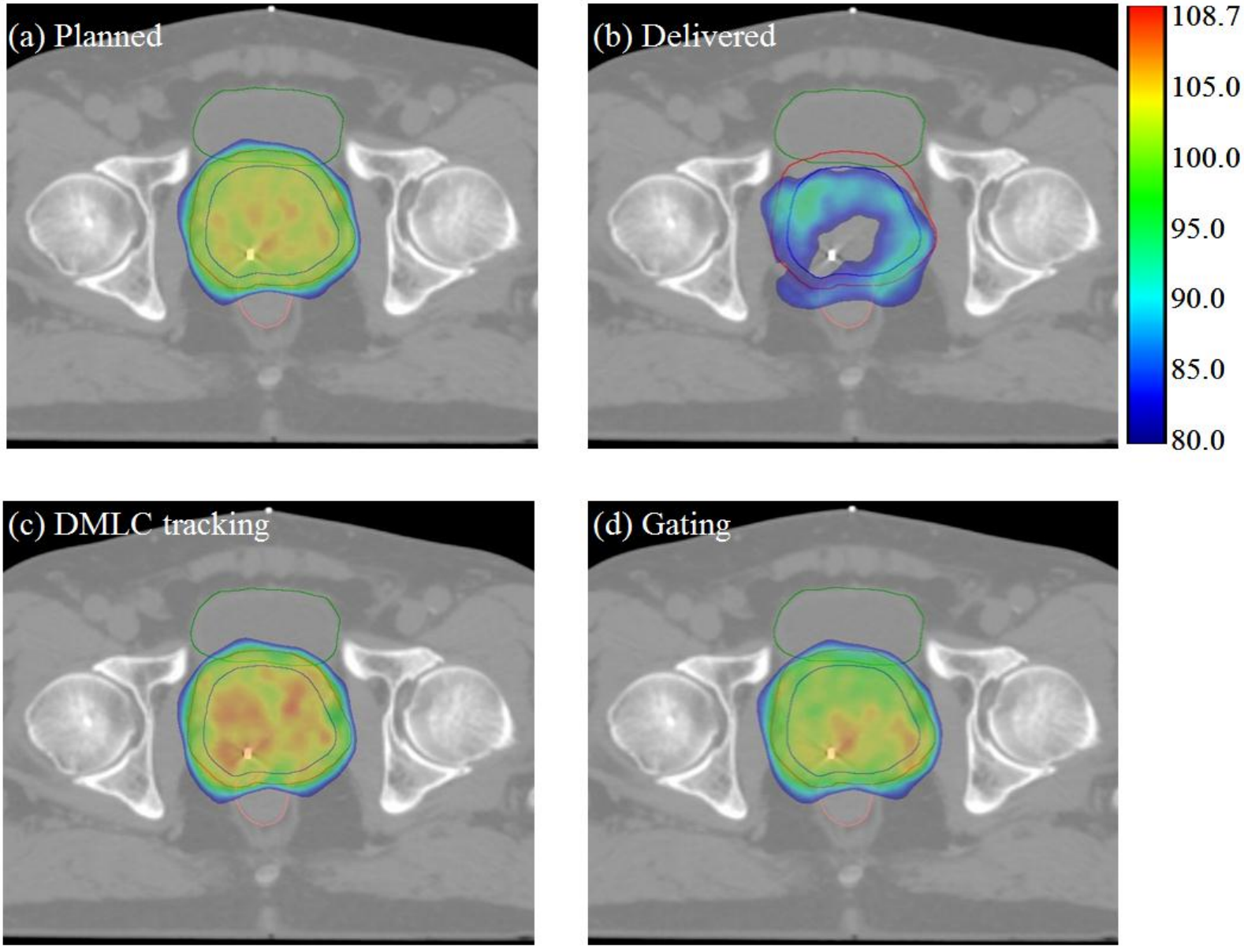
(a) Planned
(b) Delivered
108.7
105.0
100.0
95.0
90.0
85.0
80.0
(c) DMLC tracking
(d) Gating

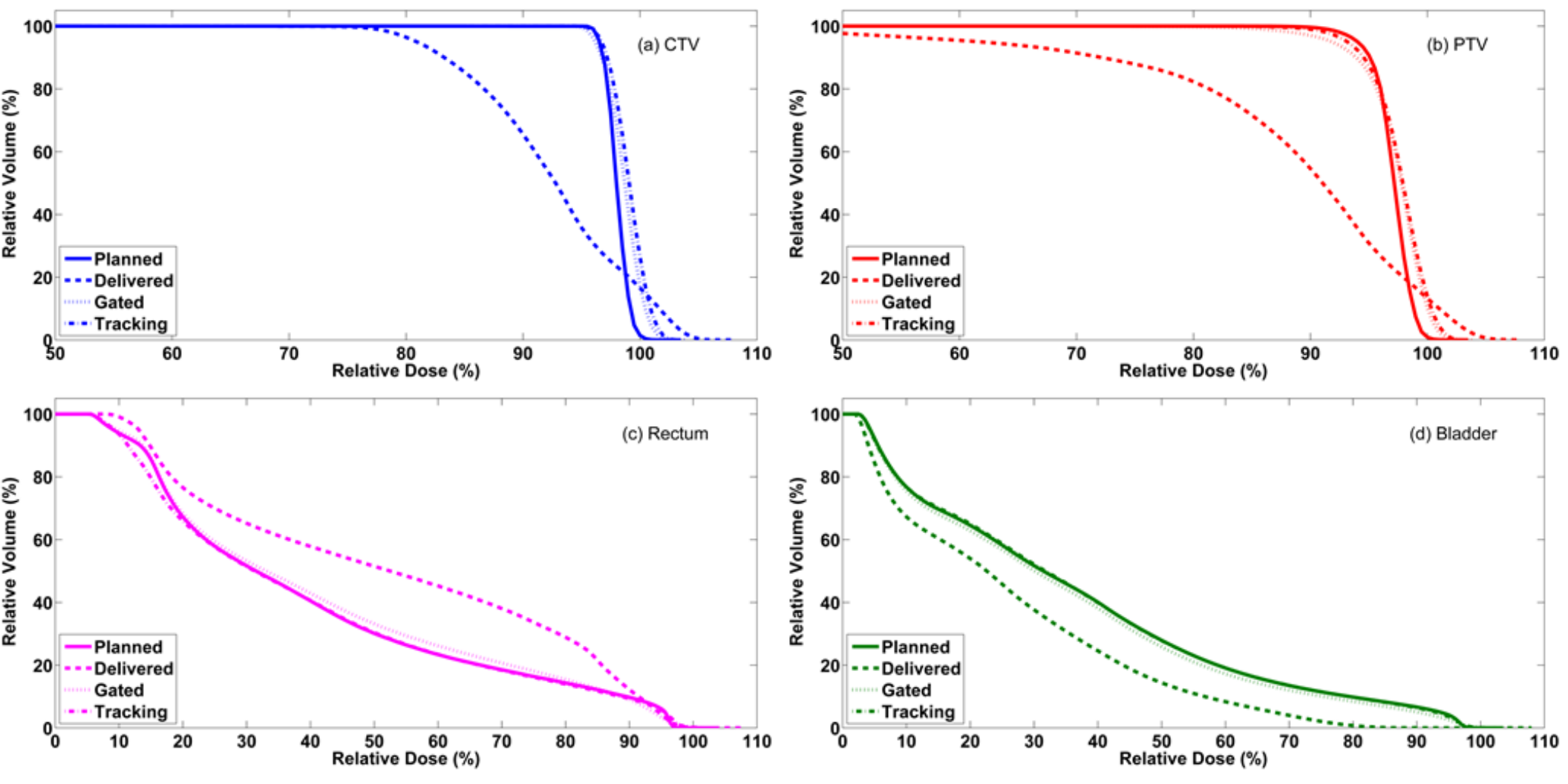
(a) CTV
(b) PTV
(c) Rectum
(d) Bladder
Planned
Delivered
Gated
Tracking
Relative Volume (%)
Relative Dose (%)

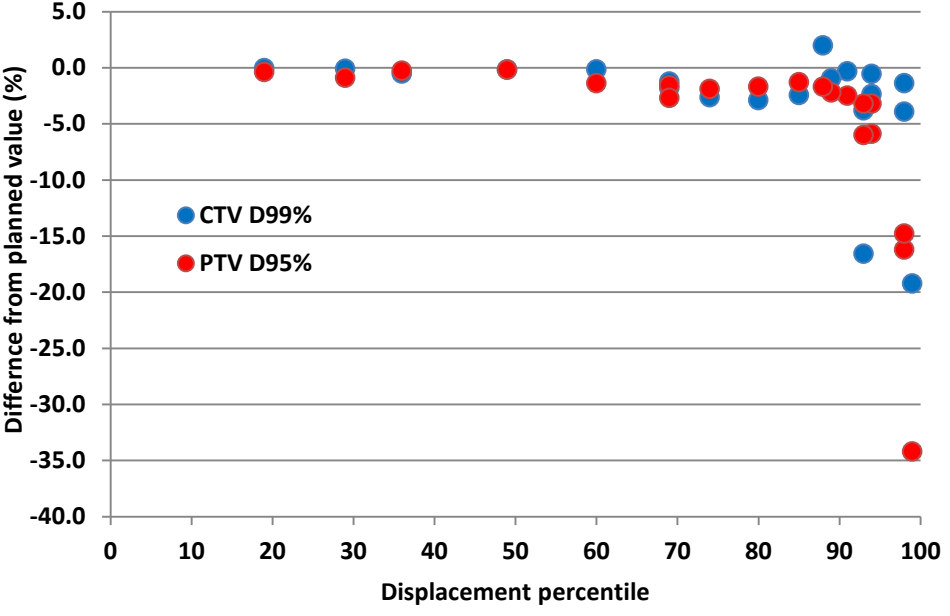
5.0
0.0
-5.0
-10.0
-15.0
-20.0
-25.0
-30.0
-35.0
-40.0
Differnce from planned value (%)
CTV D99%
PTV D95%
0
10
20
30
40
50
60
70
80
90
100
Displacement percentile

Fraction number	Motion Type	Mean Disp. (mm)	Displacement Percentile	CTV D99 (%)			PTV D95 (%)			Rectum V65 (%)			Bladder V65 (%)		
				Delivered	Tracking	Gated	Delivered	Tracking	Gated	Delivered	Tracking	Gated	Delivered	Tracking	Gated
1	Persistent	9.9	99	-19.2	-0.2	-0.7	-34.2	-0.9	-2.7	100.7	-0.3	11.5	-61.4	0.1	-10.8
2	Erratic	5.4	98	-3.9	-1.3	-3.4	-16.2	-1.6	-2.0	66.8	-1.6	-20.2	-38.0	1.7	14.0
3	Persistent	5.4	98	-1.4	-1.1	-2.6	-14.8	0.2	-1.2	16.9	1.5	-1.4	-37.3	-0.1	-1.5
4	Erratic	3.3	94	-0.6	-0.3	-2.0	-5.9	-1.0	-2.0	16.3	4.9	-2.6	23.8	0.6	1.5
5	High Freq.	3.2	94	-2.4	-2.8	-3.5	-3.2	-1.7	-3.3	-44.4	-0.1	2.1	25.9	-0.6	3.1
6	High Freq.	3.1	93	-3.8	-0.9	-3.4	-3.2	-1.1	-2.1	-18.3	0.6	-6.5	19.8	-4.4	5.4
7	Erratic	3.0	93	-16.6	-1.3	-1.2	-6.0	-1.8	-2.1	26.8	-4.4	0.0	-14.4	3.4	1.0
8	Persistent	2.7	91	-0.3	-1.3	-1.7	-2.5	-1.0	-1.6	1.6	-0.7	-1.7	-4.7	-2.2	0.3
9	Erratic	2.3	89	-1.0	-4.0	-2.1	-2.2	-1.3	-1.2	-19.5	-3.6	-11.0	14.3	-2.6	9.5
10	Persistent	2.2	88	2.0	-0.4	0.5	-1.7	0.8	-0.6	29.7	6.2	8.0	-9.0	2.3	-2.3
11	Drift	2.0	85	-2.4	-0.6	0.0	-1.3	-1.1	0.0	-23.4	2.0	-15.5	13.1	-1.2	5.6
12	High Freq.	1.7	80	-2.9	-1.8	-2.9	-1.7	-0.6	-1.7	-10.1	1.4	-10.1	8.9	2.0	8.9
13	Transient	1.5	74	-2.6	-0.9	0.0	-1.9	-0.8	-1.0	7.5	-3.2	-10.5	-4.3	3.6	4.6
14	Drift	1.4	69	-1.8	-1.2	-1.8	-1.6	-0.8	-1.6	-11.1	2.8	-11.1	5.5	-0.2	5.5
15	Transient	1.4	69	-1.2	-1.4	-1.5	-2.7	-0.7	-2.8	-6.6	-0.4	3.1	-4.2	-1.7	-4.0
16	Drift	1.1	60	-0.2	-0.1	-0.2	-1.4	-1.1	-1.4	-14.5	-6.3	-14.5	5.5	0.0	5.5
17	Stable	0.9	49	-0.2	-0.2	-0.2	-0.2	-0.2	-0.2	0.2	-1.8	0.2	9.6	0.8	9.6
18	Stable	0.8	36	-0.5	-0.3	-0.5	-0.3	-0.1	-0.3	-9.1	-4.1	-9.1	2.2	1.0	2.2
19	Stable	0.7	29	-0.1	-0.1	-0.1	-0.9	-0.7	-0.9	-9.0	-5.9	-9.0	1.5	-1.0	1.5
20	Stable	0.6	19	-0.1	-0.3	-0.1	-0.4	-0.4	-0.4	2.6	2.0	2.6	-3.6	-2.4	-3.6
		p-values compared to delivered		-	0.30	0.50	-	<0.001	0.06	-	0.68	0.53	-	0.69	0.71